BEAM LOADING EFFECTS ON THE RF CONTROL LOOPS OF A DOUBLE-HARMONIC CAVITY SYSTEM FOR FAIR*

D. Lens†, Technische Universität Darmstadt, Germany
P. Hülsmann, H. Klingbeil, GSI‡, Darmstadt, Germany.

Abstract

The effects of beam loading on the RF control loops of a double-harmonic cavity system are examined. This cavity system will be realized at the GSI Helmholtzzentrum für Schwerionenforschung in the scope of the SIS18 upgrade program. It consists of a main broadband cavity and a second harmonic narrowband cavity. The cavities comprise both an amplitude and a phase control loop. In addition, the narrowband cavity includes a control loop which controls its resonance frequency to follow the main RF frequency. After modelling the cavity system and the control loops, an analytical controller design is presented. In addition, longitudinal beam dynamics are added to the cavity model to allow a detailed simulation of the cavity-beam interaction. Realistic simulation results are given for an acceleration cycle of heavy ions to demonstrate the performance of the RF control loops.

INTRODUCTION

The construction of the new facility FAIR (Facility for Antiprotons and Ion Research, [1]) at GSI includes an upgrade of the existing SIS18 which will enable a double-harmonic operation with the main broadband cavity at the harmonic number $h = 2$ and a second narrowband cavity at $h = 4$. A typical scenario is to accelerate $^{238}U^{28+}$ ions with a particle population of $1.25 \cdot 10^{11}$ per bunch, [2]. As beam loading effects might affect the stability of the RF control loops and thus the beam stability, this work aims to show that the beam capturing and acceleration will be possible in the way it is planned. In contrast to beam loading, space charge effects are not considered, since the main focus of this work is the effect of beam loading on the stability of the RF control loops. Beam loading effects on feedback loops have been examined before, see [3]. However, the cavities considered for SIS18 cannot be regarded as sufficiently narrowband to apply these results.

SYSTEM SETUP: RF CONTROL LOOPS

Figure 1 is a schematic diagram of the planned double-harmonic system and the RF control loops. Each cavity is controlled by an individual feedback system. The controller synchronizes the phases and the amplitudes of u_{gap2} and u_{gap4} to the reference voltages u_{ref2} and u_{ref4}. The $h = 4$ cavity is kept in resonance by an additional control loop. The transfer function in the Laplace domain for the gap voltage is

$$G_{\mathrm{cav}}(s) = \frac{u_{\mathrm{gap}}(s)}{i_{\mathrm{cav}}(s)} = \frac{\frac{1}{C}s}{s^2 + \frac{1}{CR_{\mathrm{p}}}s + \frac{1}{CL_{\mathrm{p}}}} = Z_{\mathrm{p}}(s) \quad (1)$$

with $i_{\mathrm{cav}} = i_{\mathrm{gen}} - i_{\mathrm{beam}}$. The values for both cavities are listed in Table 1. The output of the amplitude and phase control is the generator current

$$i_{\mathrm{gen}} = \hat{i}_{\mathrm{gen}} \cos(\omega_{\mathrm{RF}} t + \varphi_{\mathrm{gen}}). \quad (2)$$

The amplitude $\hat{i}_{\mathrm{gen}}$ is the output of the amplitude controller $G_{\mathrm{ac}}(s)$ and depends on the difference between the desired and the detected amplitude of u_{gap}. The phase controller calculates a frequency shift based on the phase error of u_{gap}. The frequency shift is then integrated and results in

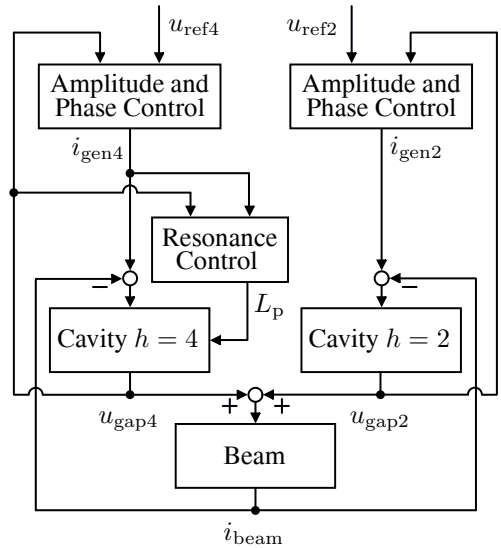

Figure 1: Schematic of the double-harmonic system.

Table 1: Cavity Parameters

	Cavity h=2	**Cavity h=4**	
C	50	395	pF
R_{p}	1.3	3	kΩ
L_{p}	506.6	[2.2 ... 100.2]*	µH
Q	0.41	[6 ... 40]	
f_{RF}	[0.4 ... 2.7]	[0.8 ... 5.4]	MHz
$\hat{u}_{\mathrm{max}}$	40	20	kV

* For the simulation, simplified parameters were assumed. The reality is more complex, because the cavities act as transformers.

* Work partly supported by Deutsche Telekom Stiftung.
† Control Theory and Robotics Lab, Landgraf-Georg-Straße 4, D-64283 Darmstadt, dlens@rtr.tu-darmstadt.de.
‡ GSI Helmholtzzentrum für Schwerionenforschung, Planckstraße 1, D-64291 Darmstadt

the phase shift φ_{gen} of the generator current. The resonance controller of the $h = 4$ cavity detects the phase error φ_{c4} between the generator current i_{gen4} and the gap voltage u_{gap4}. This error is the input of the controller $G_{\mathrm{rc}}(s)$ which produces the magnetizing current i_{m} (bias current). The magnetizing current will tune the inductivity L_{p4}, and thus the resonance frequency of the cavity, until the resonance frequency equals the RF frequency f_{RF4}. It is important to note that a significant beam current i_{beam} will disturb this process thus detuning the cavity. The dependency of L_{p4} on i_{m} is modelled as a dynamical part

$$i_{\mathrm{p}}(s) = \frac{1}{1 + T_{\mathrm{v}} s} \cdot i_{\mathrm{m}}(s) \tag{3}$$

with the time constant T_{v} and a nonlinear part

$$L_{\mathrm{p4}}(t) = L_{\mathrm{p0}} \cdot \mathrm{e}^{-k_{\mathrm{v}} \cdot i_{\mathrm{p}}(t)}. \tag{4}$$

The parameters of the pre-magnetizing circuit are shown in Table 2.

Table 2: Resonance Control Loop Parameters

T_{v}	0.25 ms	i_{m}	10 ... 800 A
L_{p0}	105.2 µH	k_{v}	$4.83 \cdot 10^{-3}\,\mathrm{A}^{-1}$

CONTROLLER DESIGN

The model shown in Fig. 1 contains five control loops, nonlinearities and, due to beam loading, a coupling of the longitudinal beam dynamics with the dynamics of the RF control loops. To enable an analytical controller design, equivalent circuit diagrams are proposed which approximate the original system. Furthermore, small beam loading is assumed in this section, thus $i_{\mathrm{beam}} \approx 0$. The impact of significant beam loading is demonstrated in the next section that shows the simulation results.

Approximation of the Cavity Dynamics

For constant values of $\hat{\imath}_{\mathrm{gen}}$ and φ_{gen}, the steady state of the gap voltage can be expressed using complex amplitudes. Considering Eq. (1), Eq. (2), and $i_{\mathrm{beam}} = 0$ leads to

$$\underline{\hat{u}}_{\mathrm{gap}} = Z_{\mathrm{p}}(j\omega_{\mathrm{RF}}) \cdot \underline{\hat{\imath}}_{\mathrm{gen}} = K_{\mathrm{p}} \cdot \hat{\imath}_{\mathrm{gen}} \mathrm{e}^{j(\omega_{\mathrm{RF}} t + \varphi_{\mathrm{gen}} + \varphi_{\mathrm{p}})}$$

with the static gain $K_{\mathrm{p}}(\omega_{\mathrm{RF}})$ and the static phase shift $\varphi_{\mathrm{p}}(\omega_{\mathrm{RF}})$ which depend on the RF frequency for the $h = 2$ cavity. As this dependency on the frequency is only minor, the controller design for the $h = 2$ cavity is carried out for $f_{\mathrm{RF2}} = 1\,\mathrm{MHz}$ to obtain constant controller gains. Changes in $\hat{\imath}_{\mathrm{gen}}$ and φ_{gen} will lead to the new steady state

$$\underline{\hat{u}}_{\mathrm{gap}} = (K_{\mathrm{p}} \hat{\imath}_{\mathrm{gen}} + K_{\mathrm{p}} \Delta\hat{\imath}_{\mathrm{gen}}) \mathrm{e}^{j(\omega_{\mathrm{RF}} t + \varphi_{\mathrm{gen}} + \Delta\varphi_{\mathrm{gen}} + \varphi_{\mathrm{p}})}.$$

The static gain of the amplitude $\Delta\hat{\imath}_{\mathrm{gen}}$ is therefore K_{p} while the gain for the phase $\Delta\varphi_{\mathrm{gen}}$ equals 1. The transition between two steady states can be approximated by the largest time constant of the cavity transfer function. This time constant T_{p} is taken as the real part of the poles of $G_{\mathrm{cav}}(s)$ that are situated nearest to the imaginary axis.

Amplitude Controller

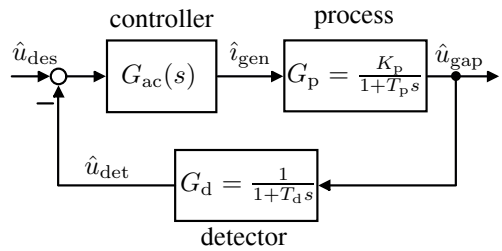

Figure 2: Equivalent circuit of the amplitude control loop.

Figure 2 shows the resulting linear amplitude control loop. The amplitude detector is approximated by the time constant $T_{\mathrm{d}} = 3.8\,\mu\mathrm{s}$. To avoid a steady-state control error, an integral controller $G_{\mathrm{ac}}(s) = \frac{K_{\mathrm{ac}}}{s}$ is chosen. This leads to the characteristic equation

$$0 = s(s + \frac{1}{T_{\mathrm{d}}})(s + \frac{1}{T_{\mathrm{p}}}) + \frac{K_{\mathrm{ac}} K_{\mathrm{p}}}{T_{\mathrm{d}} T_{\mathrm{p}}}$$

of the closed loop system. Using the root locus method, the optimal controller gain K_{ac} can be found by choosing the poles of the closed loop system.

Phase Controller

The controller design for the phase control loop is similar with one exception, namely that this process already contains an integral part. In this case, a proportional controller $G_{\mathrm{pc}}(s) = K_{\mathrm{pc}}$ is sufficient to achieve steady-state accuracy. Hence, the same procedure can be used to determine K_{pc}, using $K_{\mathrm{ac}} \mapsto K_{\mathrm{pc}}$ and $K_{\mathrm{p}} \mapsto 1$. The time constant T_{d} of the phase detector was determined to be 6 µs.

Resonance Controller

The set point to keep the $h = 4$ cavity in resonance is

$$\varphi_{\mathrm{c4}} = \measuredangle \{Z_{\mathrm{p}}(j\omega_{\mathrm{RF4}})\} \stackrel{!}{=} 0.$$

The resonance controller comprises a feedforward control to reach the set point and a feedback control for stabilization. Using Eq. (3) and Eq. (4) and linearizing around the set point leads to the transfer function

$$G_{\mathrm{p}}(s) = \frac{\varphi_{\mathrm{c4}}(s)}{i_{\mathrm{m}}(s)} = \frac{1}{1 + T_{\mathrm{v}} s} \cdot \frac{k_{\mathrm{v}} R_{\mathrm{p4}} \omega_{\mathrm{RF4}} C_4}{1 + T_{\mathrm{c}} s}.$$

Choosing a PI-controller $G_{\mathrm{rc}}(s) = K_{\mathrm{rcP}} + \frac{K_{\mathrm{rcI}}}{s}$, the largest time constant in the control loop T_{v} can be cancelled, improving the closed-loop performance.

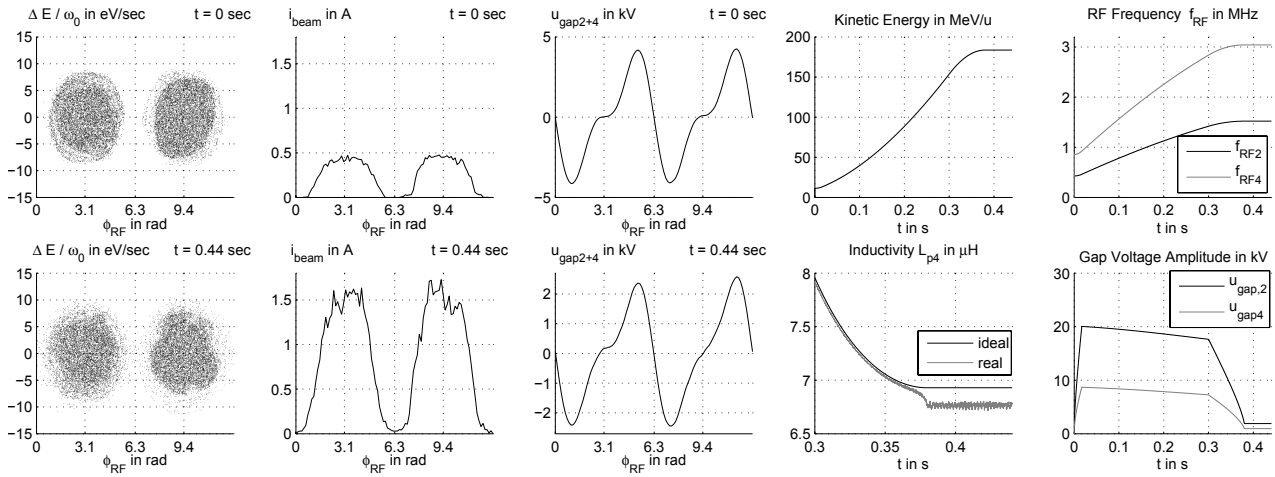

Figure 3: Simulation of the SIS18 scenario. From left to right: phase space, beam current, and total gap voltage before and after the acceleration of the beam. Kinetic energy, inductivity L_{p4}, RF frequencies and amplitudes of the gap voltages.

Table 3: SIS18 Scenario

Ion species	$^{238}\mathrm{U}^{28+}$	
SIS18 circumference	$216.72\,\mathrm{m}$	
Transition γ_{T}	5.45	
Kinetic energy (injection)	$11.4\,\mathrm{MeV/u}$	
Beam current at t =	**0 s**	**0.44 s**
Peak current	0.48 A	1.73 A
Average current	0.24 A	0.85 A
First harmonic	0.24 A	0.81 A
Second harmonic	0.04 A	0.12 A

SIMULATION: $^{238}\mathrm{U}^{28+}$ SCENARIO

The complete system including longitudinal beam dynamics was simulated for the $^{238}\mathrm{U}^{28+}$ scenario for SIS18. The coasting beam is injected at a kinetic energy of $11.4\,\mathrm{MeV/u}$ with a relative momentum spread of $\pm 10^{-3}$. After the bunching of the beam, each bunch consists of $1.25 \cdot 10^{11}$ ions, it fills $2/3$ of the bucket area. The acceleration is performed with a maximum ramping rate of the magnetic field of $4\,\mathrm{T/s}$. Figure 3 shows the simulation results of beam acceleration whereas Table 3 lists the parameters of the scenario. After the acceleration, the beam current has increased by a factor of approximately 3. The amplitudes of the gap voltages are adjusted during the acceleration to maintain a constant bucket area in phase space. Compared to injection, only about half the gap voltage is needed after acceleration. Also, the distortion of the gap voltage is higher due to the higher beam current and the lower gap voltage. The inductivity L_{p4} shows the detuning of the $h = 4$ cavity caused by the beam current. The maximum detuning is about 3 %. The phase space plots indicate a small filamentation of the beam. The simulation revealed particle losses during acceleration of $0.4\,\%$; these losses will be dominated by other loss mechanisms.

SUMMARY

The beam loading effects on the planned double-harmonic system for SIS18 have been evaluated. First, an analytical controller design for the double-harmonic cavity setup for SIS18 has been presented. Because of the complexity of the system including longitudinal beam dynamics and beam loading, equivalent circuit diagrams were introduced that approximate the dynamics of the RF control loops for the case of low beam loading. Afterwards, the controllers and the cavity dynamics were used in conjunction with a model concerning the beam dynamics to perform multi-particle simulations of the $^{238}\mathrm{U}^{28+}$ scenario. The results show that, for this typical scenario and beam current, the beam loading affects neither the stability of the control loops nor the stability of the longitudinal beam dynamics. This confirms the capability of the current design of the control loops with respect to double-harmonic operation in SIS18.

ACKNOWLEDGEMENTS

We would like to thank U. Laier (GSI) for his helpful suggestions.

REFERENCES

[1] P. Spiller et al., “Technical Design Report FAIR SIS100 Synchrotron”, GSI, March 2008.

[2] P. Hülsmann, O. Boine-Frankenheim, H. Klingbeil and G. Schreiber, “Considerations Concerning the RF System of the Accelerator Chain SIS12/18 - SIS100 for the FAIR-Project at GSI”, internal note, 2004.

[3] F. Pedersen, “Beam Loading Effects in the CERN PS Booster”, IEEE Transactions on Nuclear Science, Vol.NS-22, No.3, 1975.